ELSEVIER

Biophysical Chemistry 81 (1999) 197–205

Biophysical Chemistry

www.elsevier.nl/locate/bpc

Molecular dynamics simulations of Cu,Zn superoxide dismutase: effect of temperature on dimer asymmetry

M. Falconi[a], S. Melchionna[b], A. Desideri[a,*]

[a] *INFM and Department of Biology, University of Rome 'Tor Vergata', Via della Ricerca Scientifica, 00133 Rome, Italy*
[b] *Department of Chemistry, University of Cambridge, Lensfield Road, Cambridge, CB2 1EW, UK*

Received 10 May 1999; received in revised form 21 July 1999; accepted 21 July 1999

Abstract

Molecular dynamics simulations of solvated dimeric Cu,Zn superoxide dismutase have been carried out at four temperatures, namely 200, 225, 250 and 300 K. Analysis of the backbone-to-backbone hydrogen bonds number indicates that the symmetry observed in the two subunits at 200 K is gradually lost by heating the system. The C_α atoms displacement cross-correlation maps confirm that the asymmetric behaviour of the two subunits increases as a function of temperature. The dynamic cross-correlation of the subunits volumes indicates a fast correlation between the two subunits at 300 K, which is delayed upon lowering the simulation temperature. These results indicate that temperature plays an essential role in injecting such an asymmetry; the two subunits being asymmetric and in rapid communication at 300 K, and almost symmetric and in slow communication at lower temperatures.

Keywords: Molecular dynamics simulation; Cu,Zn superoxide dismutase; Structure–function relationship; Transition temperature; Dynamical cross-correlation

1. Introduction

Superoxide dismutases (Cu,Zn SODs) are a class of metallo-enzymes that catalyse the dismutation of superoxide into oxygen and hydrogen peroxide by alternate reduction and oxidation of a copper ion which constitutes the active redox site [1]. The functional properties of this enzyme has been extensively studied by a series of projects based on site directed mutagenesis which have shown that the catalytic rate of the enzyme is diffusion limited and that the fully conserved Arg 141 plays an essential role in both the attrac-

* Corresponding author. Tel.: +39-06-72594376; fax: +39-06-72594326.
E-mail address: desideri@uniroma2.it (A. Desideri)

0301-4622/99/$ - see front matter
PII: S0301-4622(99)00094-0

tion and the correct orientation of the negatively charged substrate anion [2–5]. Such a result has been also corroborated by numerical studies [6–9]. The three-dimensional structure of the enzyme has been thoroughly characterised by crystallographic analysis of either the oxidized and the reduced form of different eukaryotic species [10–15] showing a conserved fold constituted by two structural and chemically identical subunits of 16 kDa (Fig. 1) called Orange and Yellow in the bovine enzyme [10]. Notwithstanding the always described subunit equivalence in SOD dimers, two previous molecular dynamics (MD) studies of the whole bovine dimeric molecule in water, performed in a time window of 300 ps, have provided evidence of the occurrence of dynamical asymmetry between the two subunits [16,17]. Subsequent MD simulations of the hydrated SOD dimer [18], carried out at six different temperatures pointed out that the inter-subunit asymmetry, monitored by analyzing the Debye Waller factor of each atom, is almost absent at 200 K and increases upon heating the system.

A static asymmetry between the two monomers has been reported for the first time in an X-ray diffraction study of a single mutant (G37R) of human Cu,Zn SOD [19] found in patients with the inherited form of FALS disease, a neurodegenerative disorder characterized by the distruction of large motor neurons in the spinal cord and brain. A recent X-ray diffraction study of native bovine Cu,Zn SOD has indicated that in one of the two subunits the copper atom is preferentially reduced as a result of either a functional asymmetry between the subunits or a different accessibility of the active site channels in the crystalline state to possible reductants [20].

In order to shed light on the origin of this asymmetry we have analyzed four MD trajectories, carried out at different temperatures, of the native dimeric bovine Cu,Zn SOD selecting a number of different indicators to detect the presence of an asymmetry both in the space and in the time domain. The results indicate that at 300 K the motion of the two monomers at each instant is not symmetrical and that the asymmetry decreases at lower temperatures. Furthermore, from the time cross-correlation function of the monomer volumes, we infer the temperature dependence of the correlation times for the signal transmission across the protein interface.

2. Computational methods

2.1. Molecular dynamics

Molecular dynamics simulations of solvated

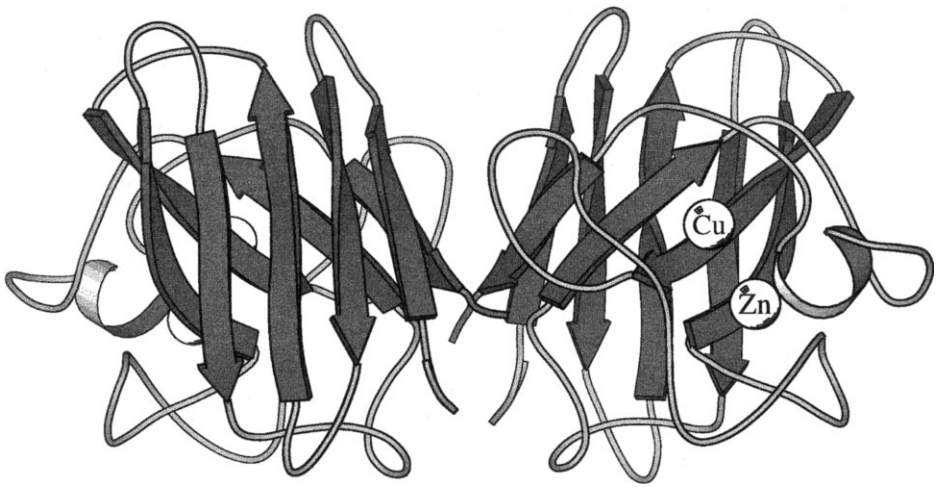

Fig. 1. Schematic view of bovine Cu,Zn superoxide dismutase. The dark grey arrows indicate the β-strands constituting the β-barrel. The three major loops and the four turns connecting the β-strands are represented as light grey thin wires. The spheres represent the metal ions. The picture was produced by using the MolScript v1.4 program [48].

bovine SOD have been performed by considering the whole dimeric protein embedded in 1847 water molecules plus four sodium counterions. This hydration level provides the necessary amount of water molecules to properly fill the simulation box so that at least two water layers are present between the protein surface and the surface of adjacent images within the periodic boundary conditions (PBC) framework [21].

The starting coordinates of the Cu,Zn SOD Orange/Yellow dimer at 2.0 Å resolution [10] were obtained from the X-ray data (entry 2sod) present in the Brookhaven Protein Data Bank [22].

The equilibrium properties of solvated SOD were sampled in the isothermal–isobaric (NPT) ensemble by using the Nosé–Hoover technique [23]. Pressure was kept fixed at 1.0 atm. The Nosé–Hoover thermostatting and barostatting coupling times were chosen at 0.4 and 10.0 ps, respectively. The MD integration time step was chosen to be 1.5 fs and the trajectories at different temperatures were propagated in time for different lengths, depending on the chosen temperature, in order to sample significantly the available phase space. In particular the trajectory at 300 K was extended up to 1260 ps while those at 250, 225 and 200 K were 250, 240 and 150 ps long, respectively.

The simulations were performed by using the parallel computer code DL-POLY developed by Smith and Forester at Daresbury Laboratory [24] with the amendments known as DL-PROTEIN [25]. We used the GROMOS [26] force field with the parameter set denoted '37c' for the protein [18], and the water molecules were represented by means of the SPC model [27].

For the active site metal clusters atomic partial charges calculated elsewhere with ab initio methods have been used [28]. The metal ions were covalently bound to their ligands but the flexibility of the active site was preserved assigning zero value to the restoring force constant of the torsion angles that describe the coordination geometry. We have used a Lennard–Jones parametrization for the non-bonding potential of zinc and copper with the surrounding atoms. The potential parameters of the zinc atom have been adopted for both metal atoms. This particular choice has been proven to be accurate enough for our purposes by previous computational studies performed by us and by other authors [16–18,29–31]. All bond lengths were kept fixed over time by using the SHAKE iterative procedure [32] with a relative bond length tolerance of 10^{-6}. A cut-off of 15 Å was used for truncation of the non-bonded interaction terms without applying any switching function due to the large cut-off used.

Electrostatic interactions were carefully computed using the Ewald sum method [21] and by computing the electrostatic contribution in reciprocal space using 8, 11 and 8 k-points in the x, y and z directions, respectively and with the Ewald convergence parameter a set to 0.195. These parameters have been chosen in order to obtain a relative accuracy in the electrostatic energy of 10^{-5}. The procedure used in the MD simulations at different temperatures has been already reported in a previous paper where the calculated and the experimental Debye–Waller factors of the hydrogen atoms have been compared [18].

The equilibration of the system at $T = 200$ K was obtained starting from the X-ray structure of SOD, relaxing the structure to 0 K by the steepest descent quenching procedure, and successively raising T until reaching 200 K in a 10-ps transient run. Finally the system has been equilibrated in the NPT ensemble during a 30-ps run with the NPT method. At this point, once the time dependence of volume and potential energy showed a stationary behaviour, the equilibrium run was carried out. In order to reach the subsequent temperature we have applied the same scheme as above, starting from the last configuration at 200 K trajectory and raising the system temperature to 225 K, and so on for all the studied temperatures.

The square configurational distance from the starting equilibrated structure as a function of time is slightly higher than 0.5 Å^2 at 200–225 K whilst the plateau values are below 1.5 Å^2 and 3.5 Å^2 at 250 and 300 K, respectively [18].

2.2. Secondary structure analysis

Data analysis of SOD has been performed on

configurations extracted every 0.1 ps. Analysis of the secondary structure of the enzyme, as a measure for the structural stability, was achieved by iteratively using the DSSP program [33]. At each temperature the subunits exhibit a stationary content of β structure indicating that the β-barrel motif of SOD, and then the overall three-dimensional fold of the protein, is conserved during each simulation. In fact, due to the globular nature of the antiparallel β-barrel motif, matching of the β structural elements in the β-barrel is possible only when the protein retains the original backbone-to-backbone hydrogen bond network and hence the correct globular folding.

2.3. Displacements cross-correlation map

The extent of correlated motions between residues has been analysed by using the displacement cross-correlation map (DCCM) which indicates the magnitude of the correlation coefficient between the C_α atoms [34]. The cross-correlation coefficients for the displacement of each pair of C_α atoms i and j is given by:

$$c_{ij} = \frac{\langle \Delta \mathbf{r}_i \cdot \Delta \mathbf{r}_j \rangle}{\sqrt{\langle \Delta r_i^2 \rangle \langle \Delta r_j^2 \rangle}} \quad (1)$$

where $\Delta \mathbf{r}_i$ is the displacement from the mean position of the ith atom and the symbol $\langle\rangle$ represent the time average over the whole trajectory.

2.4. Voronoi volume

The time evolution of the dimer and of the subunits volume has been calculated iteratively using the VOLUME program [35,36]. This program determines the volume of a polyhedron surrounding each atom in a protein when the polyhedral faces are determined by the Voronoi construction [37]. This is a geometrical construction which assigns a polyhedron, with well defined volume and surface, to each point of a discrete set of atomic positions. A Voronoi polyhedron can be seen as the generalization of the

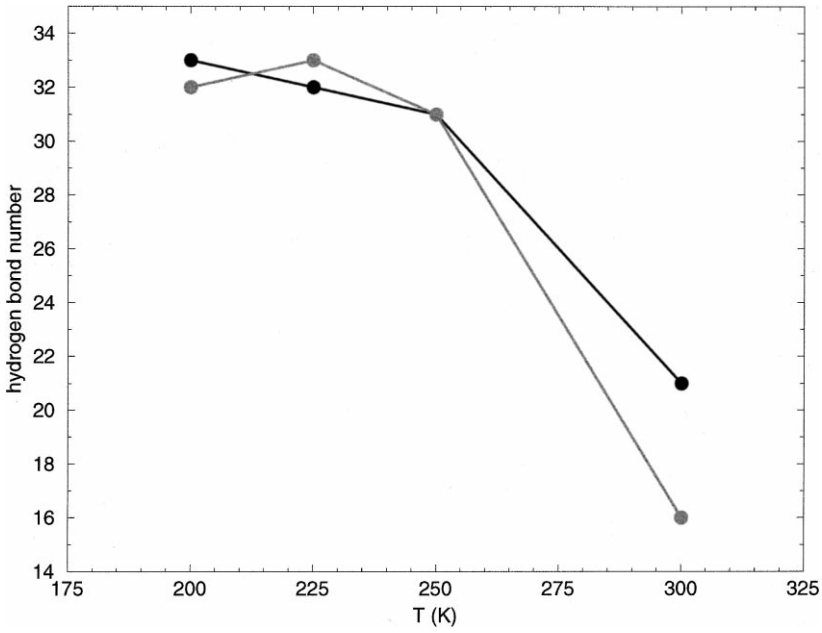

Fig. 2. Plot of the hydrogen bonds vs. temperature. The black filled circle represent the hydrogen bonds in the Orange subunit while the grey filled circle represents the hydrogen bonds in the Yellow subunit.

Wigner–Seitz cell [38] for a non-periodic set of points. A subset of points can be a residue, a domain of the secondary structure, a subunit or the whole protein. Its volume is just the sum of the volumes associated to each site of the subset.

3. Results and discussion

3.1. Hydrogen bond analysis

The persistence times of the backbone-to-backbone intraprotein hydrogen bonds (H-bonds) have been calculated. We used a geometric criterion to define the formation of an H-bond during the simulation: the hydrogen acceptor distance has to be shorter than 3.2 Å and the donor-hydrogen-acceptor angle has to be larger than 120°. In the analysis we have taken into account only the H-bonds that are detected with a persistence time larger than 80% of the total simulation time.

As shown in Fig. 2, no appreciable differences are found in the total number of H-bonds in the 200–250 K temperature range, whilst, when the temperature rises up to 300 K, the total number of H-bonds decreases and the number of H-bonds in each subunit differentiates (21 and 16 permanent H-bonds in the Orange and Yellow subunit, respectively).

3.2. Displacement cross correlation maps

Interesting results concerning the relative flexibility of each subunit may be carried out by calculating the displacement cross-correlation maps. Such plots are reported in Fig. 3A–D for the complete trajectory of the four analyzed temperatures (300, 250, 225 and 200 K, respectively).

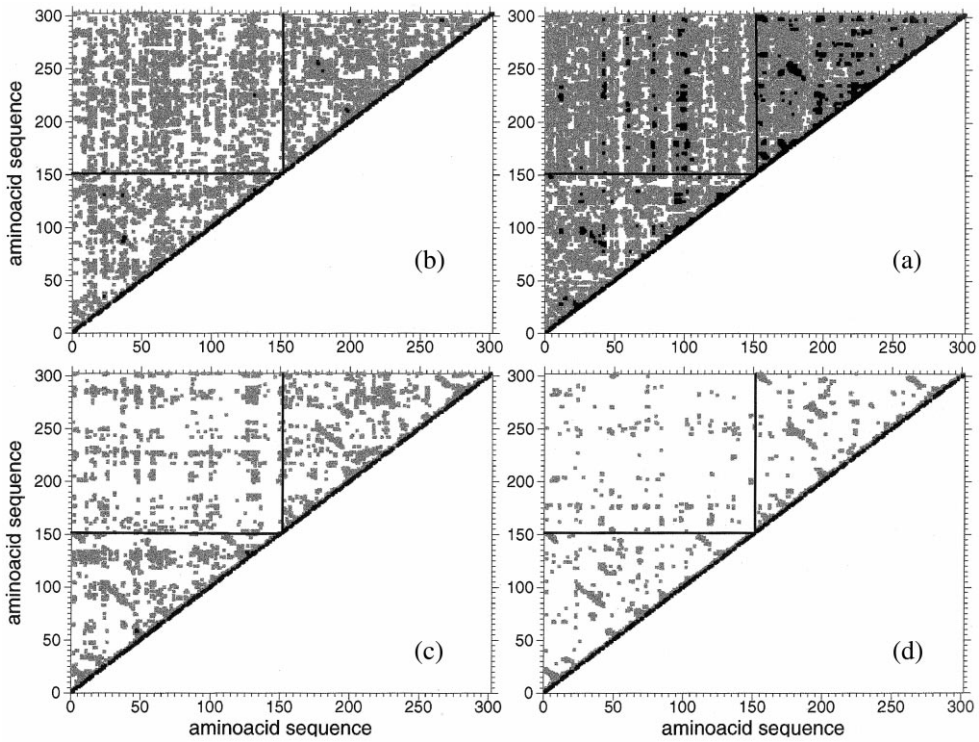

Fig. 3. Displacement cross-correlation map calculated at $T = 300$ (A), 250 (B), 225, (C) and 200 K (D). The upper-left rectangle reports the C_α inter-subunits correlations, the lower-left and upper-right triangles the C_α intrasubunit correlations for the Orange and Yellow subunit, respectively. The black squares (■) represent $0.6 \leq |c_{ij}| \leq 1.0$, while the grey squares (□) represent $0.2 \leq |c_{ij}| \leq 0.6$ (c_{ij} is defined in Eq. (1) of Computational methods).

In all cases the upper-left rectangle represents the inter-subunit positional correlation of the C_α atoms while the lower-left and the upper-right triangles display the intrasubunit positional correlations of the C_α atoms for the Orange and Yellow subunit, respectively. Correlations between C_α atoms are represented in the figure by a black spot if they range between 0.6 and 1, and by a grey spot if they range between 0.2 and 0.6. Lower correlations correspond to empty spots. A prevalence of white spaces in the DCCM matrix, as observed in the low T regime, indicates a low internal attitude to cooperative flexibility, i.e. a lack of correlation.

The intrasubunit correlations of the two SOD monomers gradually diversify upon increasing the temperature up to attain a completely different pattern at 300 K (Fig. 3A). Similarly the inter-subunit correlations increase up to reach the highest value at 300 K where the motion of the two subunits is highly correlated. DCCM maps shown in Fig. 3 were calculated by using all the simulation time available for each temperature, however the use of an identical time window of 150 ps for each trajectory gives qualitatively the same results.

3.3. Subunit volumes cross-correlation

The Voronoi volumes of the protein dimer for each protein subunit have been calculated at the four analyzed temperatures. The total dimer volume is almost temperature independent from 200 up to 250 K and corresponds to a volume of approximately 40 600 A^3, whilst at 300 K the total volume increases to a value of approximately 41 400 A^3.

We have analyzed the time evolution of the dynamic cross correlation between the volume V_O and V_Y of the Orange and Yellow subunit, respectively, by following the normalized dynamic cross-correlation $C_{V_OV_Y}(t)$ defined as:

$$C_{V_OV_Y}(t) = \frac{\langle \Delta V_O(t)\Delta V_Y(0)\rangle}{\sqrt{\langle \Delta V_O^2\rangle\langle \Delta V_Y^2\rangle}} \qquad (2)$$

where $\Delta V(t) = V(t) - \langle V\rangle$ is the instantaneous volume displacement from the average value, and the cross-correlation function is computed as

$$\langle \Delta V_O(t)\Delta V_Y(0)\rangle = \frac{1}{M-t}\sum_{\tau=0}^{M-t} \Delta V_O(t+\tau)\ \Delta V_Y(\tau),$$

where M is the total number of volumes collected. The cross-correlation function is defined such that $|C_{V_OV_Y}(t)| \le 1.0$ and $\lim_{t\to\infty} C_{V_OV_Y}(t) = 0$ for the statistical independence of the volumes at large times.

The meaning of $C_{V_OV_Y}(t)$ is that if V_O and V_Y are independent variables then their dynamic cross-correlation will be zero at all times within the uncertainty due to finite sampling. If an increase in V_O is accompanied by an increase in V_Y or vice versa at time t, then the cross-correlation value at that time will be positive, whilst if an increase in V_O is accompanied by a decrease in V_Y or vice versa, the cross-correlation value at that time will be negative. The value of the function at $t = 0$, called the static correlation coefficient, quantifies the extent of the instantaneous correlation between the two volumes.

As shown in Table 1 the static correlation coefficient has the largest value for the trajectory at 300 K, indicating the occurrence of an instantaneous correlation between the two subunits, whilst it decreases at lower temperatures reaching a value close to zero for the 200 K trajectory. At $T = 300$ K the values of $C_{V_OV_Y}(t)$ rapidly decays around zero (Fig. 4) indicating a fast memory loss between the subunit volumes whilst at lower temperatures the fast decays disappear. The observation of a low frequency and large amplitude wave suggests the existence of a long wavelength dynamical correlation. However, at each temperature the observed dynamical correlations do not show relevant features in the time scale above 50 ps, so that our reported time window exhibits

Table 1
Static cross-correlation values of inter-subunit Voronoi volumes

Temperature (K)	Correlation value ($t = 0$)
300	0.381
250	0.231
225	0.036
200	0.003

qualitatively all the time scales involved in the volume cross-correlation. Lowering the temperature induces large oscillating values of $C_{V_O V_Y}(t)$ corresponding to slow and persistent dynamic correlation between the subunits. Our results indicate that from $T = 300$ K to $T = 200$ K the instantaneous correlation between the two subunits is gradually eliminated and it is substituted by a delayed oscillating correlation.

4. Conclusions

Analysis of the molecular dynamics trajectories indicates that the dynamical behaviour of the SOD dimer is highly temperature-dependent. In particular at 300 K the two monomers display an inter-subunit asymmetry, as evidenced by the analysis of the H-bonds network, that decreases upon lowering the temperature. Moreover, the DCCM maps indicate that at 300 K the dimer is highly asymmetric and that the two subunits are strongly correlated. Coherently, at high temperature the Voronoi volumes of the two subunits show a large static and an almost absent dynamic correlation. On the other hand, at lower temperatures, the DCCM maps show a low degree of correlation which is accompanied by a time de-

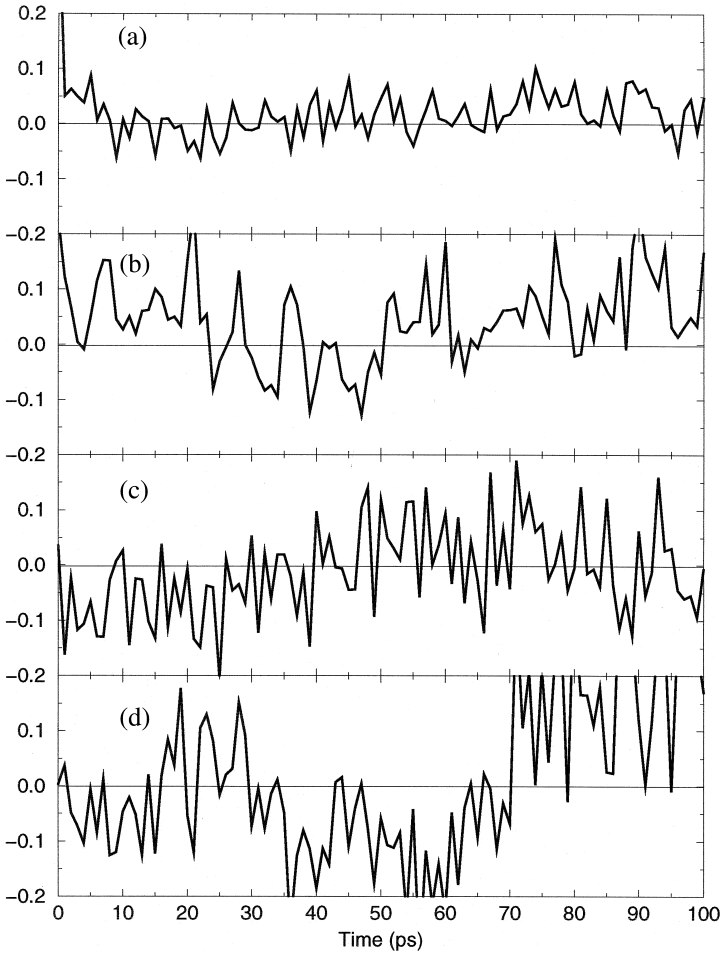

Fig. 4. Dynamic cross correlation between the Voronoi volume of Orange and Yellow subunit at: $T = 300$ (A); 250 (B); 225 (C); and 200 K (D).

layed correlation of the Voronoi volume of the two subunits. At the lowest temperature, i.e. 200 K, the two subunits are almost completely symmetric and display a slight and slow mechanical interaction. Analysis of the data of Fig. 4 indicates that communication between the subunits in the high temperature regime is represented by an instantaneous process that takes place at times less than 5 ps, whereas at low temperatures it is mediated by a mechanical stress of the monomers that communicates across the protein interface in a time range of approximately 50 ps. These values must be considered qualitative since we are not able to precisely quantify the error bars in the correlation function with the available MD data. In fact from theoretical arguments we can only predict the $t^{1/2}$ growth of the numerical uncertainty with time [39]. Thus, we expect the large time regime to be strongly affected by the numerical error. However, the trend is unambiguous and the oscillatory behaviour is unlikely to originate from the MD barostat. In fact at all different temperatures we have chosen the same piston coupling time (10 ps), much smaller than the observed oscillation period ($\cong$ 50 ps).

The description coming from our simulation study indicates that the two subunits are asymmetric and in rapid communication at 300 K, on the other hand at lower temperatures the two subunits are almost symmetric and in slow communication. The aim of our work was not to identify a transition temperature but to show that the asymmetry between the two subunits is temperature-dependent. The data of Figs. 3 and 4 indicate that such an asymmetry already starts at 225 K and that it is clearly detectable at 250 K. This temperature-dependent behaviour correlates well with a neutron scattering study of hydrated SOD as a function of temperature [40], which indicates that the protein up to approximately 200 K is characterized by harmonic motions, whilst above 200 K anharmonic contributions are injected. This experimental behaviour has been observed for other macromolecules where the temperature mediated dynamical transition influences the functionality of the protein modifying the enzyme flexibility that is required for the catalytic function [41,42]. In the case of Cu,Zn SOD, our work suggests that the anharmonic regime is coupled to the inter-subunit asymmetry, although nothing may be inferred about functionality. A recent study has shown, at least for the enzyme glutamate dehydrogenase, the absence of any correlation between anharmonic motion and activity, since the enzyme remains active below the dynamical transition observed at approximately 220 K, i.e. at temperatures where no harmonic motion is detected [43].

An important point, in the case of Cu,Zn SOD, would be to understand if the asymmetry observed at 300 K implies an alternate functioning of the two subunits. The experimental evidence for an alternate function of the SOD dimer has been provided in a study carried out on a previously freeze dried sample [44] and a conformational communication between the two subunits has been reported to occur in the process of metal reconstitution of the copper depleted enzyme [45,46]. The recent observation that in the bovine enzyme one subunit is reduced faster than the other indicates a potential functional asymmetry between the two subunits [20].

The asymmetric behaviour can be modulated by mutations as shown by the static inter-subunit asymmetry observed in single SOD mutant related to FALS disease [19]. MD simulation has been shown to be able to detect different flexibility introduced by specific mutations as shown by a comparative MD study carried out on native *Xenopus laevis* Cu,Zn SOD and on a mutant, having four charged and highly conserved residues neutralised [47]. These results indicate that Cu,Zn SOD internal dynamics is an important property to be monitored and that it may become a diagnostic parameter for understanding how to modulate its enzymatic function.

Acknowledgements

This project has been supported by the National Institute for the Physics of the Matter (INFM) project PRA MACROREC. S.M. acknowledges support from a Leverlhulme trust.

References

[1] J.V. Bannister, W.H. Bannister, G. Rotilio, CRC Crit. Rev. Biochem. 22 (1987) 111.
[2] C.L. Fisher, D.E. Cabelli, J.A. Tainer, R.A. Hallewell, E.D. Getzoff, Proteins 19 (1994) 34.
[3] C.L. Fisher, D.E. Cabelli, R.A. Hallewell et al., Proteins 29 (1997) 103.
[4] F. Polticelli, G. Bottaro, A. Battistoni et al., Biochemistry 34 (1995) 6043.
[5] F. Polticelli, A. Battistoni, P. O'Neill, G. Rotilio, A. Desideri, Protein Sci. 7 (1998) 1.
[6] I. Klapper, R. Hagstrom, R. Fine, K. Sharp, B. Honig, Proteins 1 (1986) 47.
[7] J.J. Sines, S.A. Allison, J.A. McCammon, Biochemistry 29 (1990) 9403.
[8] B.A. Luty, S. El Amrani, J.A. McCammon, J. Am. Chem. Soc. 115 (1993) 11874.
[9] A. Sergi, M. Ferrario, F. Polticelli, P. O'Neill, A. Desideri, J. Phys. Chem. 98 (1994) 10554.
[10] J.A. Tainer, E.D. Getzoff, K.M. Beem, J.S. Richardson, D.C. Richardson, J. Mol. Biol. 160 (1982) 181.
[11] Y. Kitagawa, N. Tanaka, Y. Hata et al., J. Biochem. 109 (1991) 477.
[12] K. Djinovic, G. Gatti, A. Coda et al., J. Mol. Biol. 225 (1992) 791.
[13] H.E. Parge, R.A. Hallewell, J.A. Tainer, Proc. Natl. Acad. Sci. USA 89 (1992) 6109.
[14] K. Djinovic-Carugo, A. Coda, A. Battistoni et al., Acta Crystallog. D52 (1996) 176.
[15] N.L. Ogihara, H.E. Parge, J. Hart et al., Biochemistry 35 (1996) 2316.
[16] M. Falconi, R. Gallimbeni, E. Paci, J. Comput-Aided Mol. Design. 10 (1996) 490.
[17] G. Chillemi, M. Falconi, A. Amadei, G. Zimatore, A. Desideri, A. Di Nola, Biophys. J. 73 (1997) 1007.
[18] S. Melchionna, M. Falconi, A. Desideri, J. Chem. Phys. 108 (1998) 6033.
[19] P.J. Hart, H. Liu, M. Pellegrini et al., Protein Sci. 7 (1998) 545.
[20] M.A. Hough, S.S. Hasnain, J. Mol. Biol. 287 (1999) 579.
[21] M.P. Allen, D.J. Tildesley, Computer Simulation of Liquids, Clarendon Press, Oxford, 1987.
[22] F. Bernstein, T. Koetzle, G. Williams et al., J. Mol. Biol. 112 (1977) 535.
[23] S. Melchionna, G. Ciccotti, J. Chem. Phys. 106 (1997) 195.
[24] W. Smith, T.R. Forester, J. Mol. Graph. 14 (1996) 136.
[25] S. Melchionna, A. Luise, M. Venturoli, S. Cozzini, in: M. Voli (Ed.), DLPROTEIN a Molecular Dynamics Package to Simulate Biomolecules (Science and Supercomputing at Cineca: report 97), Cineca Supercomputing Group, 1998, p. 496.
[26] W.F. van Gunsteren, H.J.C. Berendsen, GROMOS Manual, University of Groningen, Groningen, 1987.
[27] H.J.C. Berendsen, J.P.M. Postma, W.F. van Gunsteren, J. Hermans, in: B. Pullmann (Ed.), Intermolecular Forces, Riedel, Dordrecht, 1981, p. 331.
[28] J. Shen, C.F. Wong, S. Subramaniam, T.A. Albright, J.A. McCammon, Comp. Chem. 11 (1990) 346.
[29] J. Shen, S. Subramaniam, C.F. Wong, J.A. McCammon, Biopolymers 28 (1989) 2085.
[30] J. Shen, J.A. McCammon, Chem. Phys. 158 (1991) 191.
[31] Y. Wong, T.W. Clark, J. Shen, J.A. McCammon, Mol. Simul. 10 (1993) 277.
[32] J.P. Rickaert, G. Ciccotti, H.J.C. Berendsen, J. Comp. Phys. 23 (1977) 327.
[33] W. Kabsch, C. Sander, Biopolymers 22 (1983) 2577.
[34] J.A. McCammon, S.C. Harvey, Dynamics of Proteins and Nucleic Acids, Cambridge University Press, London, 1987.
[35] F.M. Richards, J. Mol. Biol. 82 (1974) 1.
[36] F.M. Richards, Methods Enzymol. 115 (1985) 440.
[37] G.F. Voronoi, Z. Reine Angew. Math. 134 (1908) 198.
[38] N.W. Ashcroft, N.D. Mermin, Solid State Physics, Saunders College, Philadelphia, 1976.
[39] R. Zwanzig, N.K. Ailawadi, Phys. Rev. 182 (1969) 280.
[40] C. Andreani, A. Filabozzi, F. Menzinger, A. Desideri, A. Deriu, D. Di Cola, Biophys J. 68 (1995) 2519.
[41] B.F. Rasmussen, A.M. Stock, D. Ringe, G.A. Petsko, Nature 357 (1992) 423.
[42] M. Ferrand, A.J. Dianoux, W. Petry, G. Zaccai, Proc. Natl. Acad. Sci. USA 90 (1993) 9668.
[43] R.M. Daniel, J.C. Smith, M. Ferrand, S. Hery, R. Dunn, J.L. Finney, Biophys. J. 75 (1998) 2504.
[44] E.M. Fielden, P.B. Roberts, R.C. Bray et al., Biochem. J. 139 (1974) 49.
[45] A. Rigo, P. Viglino, L. Calabrese, D. Cocco, G. Rotilio, Biochem. J. 161 (1977) 27.
[46] A. Rigo, P. Viglino, M. Bonori, D. Cocco, L. Calabrese, G. Rotilio, Biochem. J. 169 (1978) 277.
[47] M. Falconi, F. Venerini, A. Desideri, Biophys. Chem. 75 (1998) 235.
[48] P.J. Kraulis, J. Appl. Cryst. 24 (1991) 946.